

# Threshold non-linear absorption in Zeeman transitions.

Andal Narayanan<sup>1,\*</sup>, Abheera Hazra<sup>1</sup>, and S. N. Sandhya<sup>2</sup>

<sup>1</sup>*Raman Research Institute, Sadashivnagar, Bangalore, INDIA 560 080*

<sup>2</sup>*Department of Physics, IIT Kanpur, Kanpur, INDIA 208 016*

(Dated: June 29, 2009)

We experimentally study the absorption spectroscopy from a collection of gaseous  $^{87}\text{Rb}$  atoms at room temperature irradiated with three fields. Two of these fields are in a pump probe saturation absorption configuration. The third field co-propagates with the pump field. The three fields address Zeeman degenerate transitions between hyperfine levels  $5S_{1/2}, F=1$  and  $5P_{3/2}, F=0, F=1$  around the D2 line. We find a sub-natural absorption resonance in the counter-propagating probe field for equal detunings of all the three fields. The novel feature of this absorption is its abrupt onset in the vicinity of  $5P_{3/2}, F=0$ , as the laser frequency is scanned from  $5P_{3/2}, F=0$  to  $5P_{3/2}, F=1$ . The experimental results are compared with the theory modeled after a four level system. There is a qualitative agreement between our theory and experiment. We find the threshold absorption to be a result of the off-resonant interaction of the strong field with nearby hyperfine levels.

PACS numbers: 32.80.Qk, 42.50.Gy,

## I. INTRODUCTION

The absorption spectrum of a driven degenerate two level system (DTLS) is shown [1] to be radically different from the usual Mollow triplet corresponding to a pure two level system. The atomic coherence induced by multi-photon interactions in DTLS results in a competition between constructive or destructive quantum interference which gives rise to subnatural width resonances (SNWR) [2]. The resonance could manifest as induced absorption (EIA), transparency (EIT), or even gain, depending on the polarization, intensity and detunings of the driving fields. The line shapes are further influenced on whether the system is closed (cyclic) or open [5], velocity selection [7], and the presence of small polarization admixtures [6]. Akulshin et al., [3] have extensively studied DTLS involving various ground state and excited state hyperfine levels both theoretically and experimentally. They arrive at a criteria [4] for the occurrence of EIA in DTLS, namely (i)  $F_e = F_g + 1$ , (ii) the ground to excited state transition is closed and (iii)  $F_g > 0$ .

The occurrence of EIA has been attributed to the transfer of coherence from excited state to the ground state [8] and also to the transfer of population [9]. Inhibition of EIA due to excited state decoherence has also been reported experimentally [10]. Most of these studies involve the interaction of DTLS with two driving fields. Multiple driving fields interacting with DTLS has been reported in the context of coherent hole burning [11] where the same transition is addressed by a saturating beam and a probe.

In this paper we experimentally study the occurrence of sub-natural absorption resonances in the counter probe during a three field irradiation of gaseous, room temperature  $^{87}\text{Rb}$  atoms. These three fields address Zeeman

degenerate transitions in a DTLS configuration. These resonances arise as a result of dark resonances created by the co-propagating fields, inducing a higher order, off-resonant absorption to neighbouring hyperfine levels in the counter field. Since the intensity regime of the probe in which the absorption is seen is well below saturation, we do not expect coherent population oscillations [12] to affect the absorption line shape [7]. The absorption is studied as a function of detunings of the three driving fields. We find, as a function of this detuning, the existence of a sharp threshold where the absorption begins to show up. We compare our experimental results with a theoretical model comprising of a modified 'N' system which has contributions from a double lambda system and double 'V' system depending on the detunings of the laser beams. The modeling reproduces the threshold behaviour very clearly.

## II. EXPERIMENT

### A. Level Structure

The hyperfine levels around the D2 line of  $^{87}\text{Rb}$  is shown in Figure 1(a). Figure 1(b) shows the Zeeman sub-levels of  $F=1$  ground hyperfine state and that of excited hyperfine states  $F=0', 1'$  [23] relevant for the experiment described here.

### B. Experimental setup

Three beams L1, L2 and L3, derived from a single laser irradiate a room temperature sample of  $^{87}\text{Rb}$  atoms. The laser is an External Cavity Diode Laser (ECDL) with a line width typically around 1 MHz operating around the D2 line at 780 nm. The laser frequency is scanned around the hyperfine manifold starting from ground state  $5S_{1/2}, F=1$  to excited states  $5P_{3/2}, F=0'$

---

\*Electronic address: andal@rri.res.in

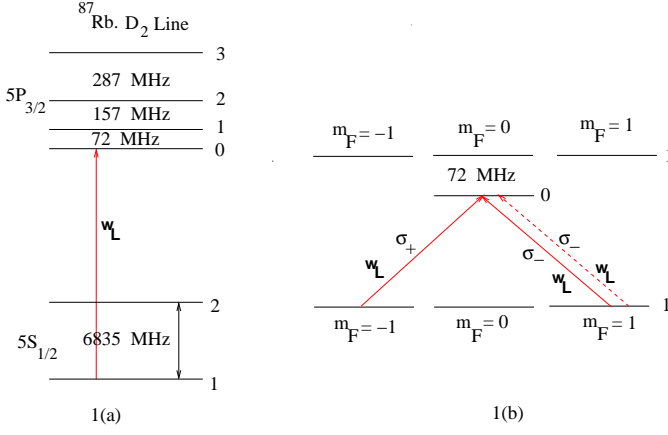


FIG. 1: Level Scheme.

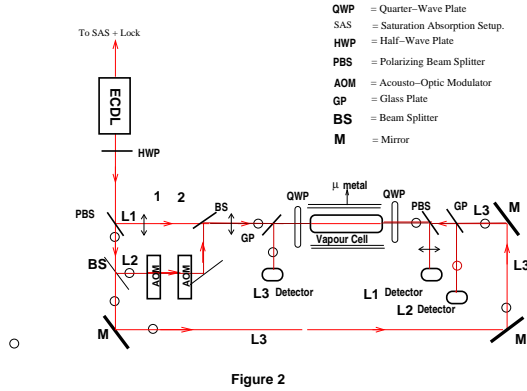


FIG. 2: Schematic of the experimental setup.

and  $5P_{3/2}, F = 1'$ . The laser frequency is monitored through a saturation absorption setup as indicated in Figure 2. A phase sensitive feed back mechanism is employed to lock the frequency of the laser to any one of the excited states. As shown in Figure 2, L1 and L2 are collinear and co-propagating and L3 counter-propagates to both L1 and L2. L1 is typically of higher intensity than L2 with intensity ranging between  $1 I_s$  and  $5 I_s$  where  $I_s$  is the saturation intensity for the transition  $5S_{1/2}, F = 1$  and  $5P_{3/2}, F = 0'$ . L2 has intensity in the range of  $0.1 I_s$  to  $0.5 I_s$ . L3 has the least intensity ranging between  $0.1 I_s$  and  $0.01 I_s$ . All the three beams being derived from a single laser have the same laser frequency  $\omega_L$ . At any given  $\omega_L$ , the L2 beam can be ramped over a frequency range of  $\pm 10$  MHz around  $\omega_L$ , by a combination of two Acousto-Optic-Modulators (AOMs in Figure 2). Thus for a given detuning  $\delta_{10}$ , measured from  $5P_{3/2}, F = 0'$  level, the L2 beam, through the AOMs can scan a width of  $\pm 10$  MHz about  $\delta_{10}$ . The experiment consists of recording the transmitted intensities of all three beams using fast photodiodes. The transmitted intensities show two kind of variations. One of these is due to changing  $\omega_L$ . These variations mimic the standard saturation absorption variations in the transmission of counter-propagating L3 probe, for appropriate inten-

sity ratios of L1 and L3. But because of the presence of L2 co-propagating with L1, at every  $\omega_L$ , the condition for a two-photon Raman resonance is satisfied between L1 and L2. The results in transmission changes in L2 and L3 which are very different from a standard saturation experiment. In fact, during the  $\pm 10$  MHz frequency scan of L2 centered at  $\omega_L$ , we see enhanced transmission of L2 due to EIT as expected. As the AOM scan rate is faster than the scan of laser frequency  $\omega_L$ , the spectral features are dominated by features during the faster frequency scan in the narrow bandwidth centered around  $\delta_{10}$ . The slower scan of the laser frequency  $\omega_L$  results in a varying background.

The L1 and L2 beams are orthogonally polarized with the quantization axis as the direction of propagation and the L3 beam is polarized similar to the L1 beam. The vapor cell containing gaseous Rubidium atoms in their natural isotopic abundance, is covered with three layers of  $\mu$  metal shield. The residual field is in the range of 10 to 20 milligauss inside the cell.

### C. Level structure for multi-photon transitions

The three laser beams L1, L2 and L3 can drive Zeeman degenerate transitions as shown in Figure 3. Figure 3(a) shows transitions between the Zeeman sublevels of  $5S_{1/2}, F = 1$  and  $5P_{3/2}, F = 0'$ . The laser beams L1 (shown thick) and L2 which are oppositely polarized form a  $\Lambda$  system with the magnetic hyperfine levels  $m_F = \pm 1$  of ground state  $F = 1$  and the excited state level  $F = 0'$ . The beam L3 is counter propagating to L1 and L2 and hence there is a frequency offset in the atomic rest frame due to the thermal motion. L3 connects the same set of levels as L1, shown here in dotted lines. Figure 3(b) show transitions between the Zeeman sublevels of  $5S_{1/2}, F = 1$  and  $5P_{3/2}, F = 1'$ . For oppositely circularly polarized L1 and L2 this gives rise to a  $\Lambda$  and a 'V' configuration for EIT. Even here because the L3 beam (shown in dotted lines) is counter to L1 and L2, it does not take part in the transparency effect.

Because of the presence of several velocity classes of atoms at room temperature, even when the laser is addressing resonantly the transition shown in Figure 3(a), it is off-resonantly addressing transitions in the  $F = 1'$  manifold and vice-versa. This effect is most prominent for the L1 laser which has a higher intensity than L2 and L3. So a realistic picture of possible laser transitions is shown in Figure 3 (c). Here the dot-dash line indicates the transitions addressed by L1 laser off-resonantly.

## III. RESULTS AND DISCUSSION

Figure 4 shows the typical transmitted intensities of L1 and L3 beams for various detunings  $\delta_{10}$ . As stated

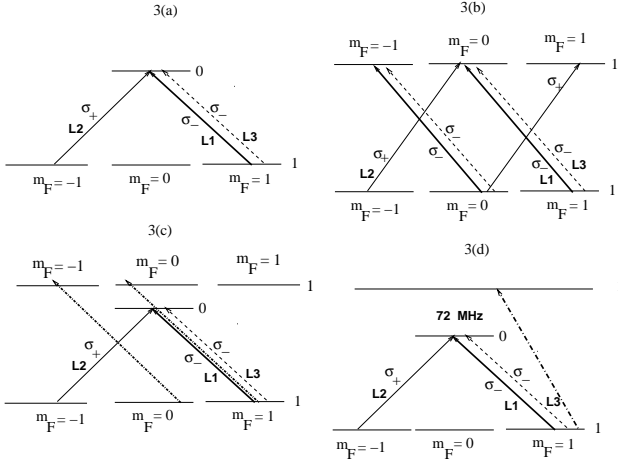


FIG. 3: Thick line denotes L1 laser. Dotted line denotes L3 laser. Dot-Dash line denotes off-resonant transitions of L1 laser. L2 is denoted by an ordinary line. (a) Zeeman transitions between  $F = 1$  and  $F = 0'$ . (b) Zeeman transitions between  $F = 1$  and  $F = 1'$ . (c) Off-resonant transitions of the L1 laser when it is addressing  $F = 1$  to  $F = 0'$  transition. (d) N system with resonant and off-resonant transitions.

before, L1, L2 and L3 beams have the same detuning  $\delta_{10}$  as they are derived from the same laser. The L2 beam scans, at every detuning  $\delta_{10}$ , a frequency range of  $\pm 10 \text{ MHz}$  centered around  $\delta_{10}$ . Trace B of Figure 4(a) shows the ramp voltage scan applied to the AOMs in the path of L2 resulting in a frequency scan of a  $\pm 10 \text{ MHz}$  of L2, centered around a given  $\delta_{10}$ . On either side of these AOM frequency scans are shown Traces A and C. Traces A and C show the transmitted intensity profiles of L2 and L3 respectively, during the scan of L2 centered around a given value of  $\delta_{10}$ . As can be seen from trace A, L2 shows increased transmission over the background, whenever L1 and the scanned L2 are at the same detuning, satisfying the two photon resonance condition for EIT. The EIT window is typically of 1 - 2 MHz width. On the other hand, the transmitted intensity of L3 given in Trace C shows a sharp absorption resonance, at the very position at which L2 shows EIT transmission resonances. The width of this absorption is sub-natural ranging between 300 KHz to 800 KHz. The graph of Trace C has been amplified 6 times for clear representation in this combined graph. Since this absorption in L3 occurs whenever the co-propagating L1 and L2 satisfy the two-photon EIT condition, it implies a higher order absorption mechanism for L3 absorption. In fact, a related three-photon absorption was seen by us in an N level scheme [13] for similar geometry of beams. The novelty of such a feature here, for Zeeman degenerate transitions, is its abrupt onset [14] as is shown in Figure 5.

Shown in Figure 5 are Traces A and C from the same experimental run as it is for Figure 4 but in a different region of  $\delta_{10}$  around  $F = 0'$ . As can be seen from this graph, while Trace A remains qualitatively unchanged even in this region, Trace C shows abrupt disappearance

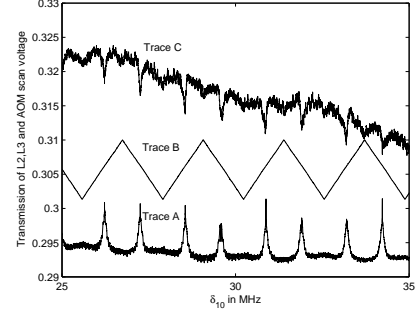


FIG. 4: Trace B denotes the ramp voltage going to the AOM of the L2 beam resulting in a frequency scan of  $\pm 10 \text{ MHz}$  around a given  $\delta_{10}$ . Trace A denotes L2 transmission showing increased transmission whenever the two co-propagating L1 and the scanned L2 meet the two-photon resonance condition for EIT. Trace C shown decreased transmittance (absorption) of the counter L3 beam at two-photon resonance

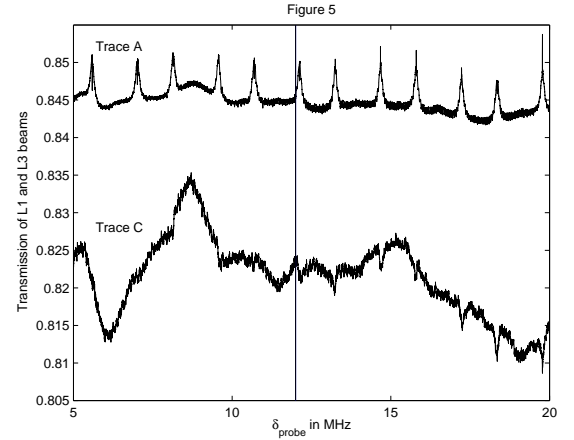


FIG. 5: Traces A and C of Figure 4 shown in a region of  $\delta_{10}$  around 12 MHz showing abrupt onset of L3 absorption resonance

of the absorption feature below  $\delta_{10} < 12 \text{ MHz}$  marked by the vertical line in the figure. For all values of  $\delta_{10}$  below this value, there is no narrow absorption seen in Trace C. The background absorption of L3 in this region show changes which is not correlated with the appearance of EIT feature in the L2 field (Trace A). We have estimated for this graph that the narrow absorption disappears within a 5 MHz change of  $\delta_{10}$  to the left of the vertical line. Conversely, we can say that the nonlinear absorption in L3 has an abrupt onset around  $\delta_{10} = 12 \text{ MHz}$ .

For the sake of clarity we have shown in Figures 6(a) and 6(b), the entire region of  $\delta_{10}$  values extending upto  $-35 \text{ MHz}$ . The narrow absorption feature in L3 (Trace C) is totally absent in this region. Only beyond the vertical line do we see the onset of this absorption. On the contrary Trace A, of this figure, representing L2 transmission, continues to show the EIT feature for all values of

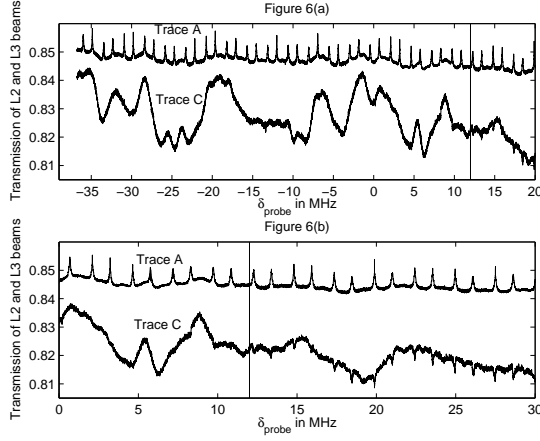


FIG. 6: (a) Absence of L3 absorption resonance to the left of the vertical line (Trace C) for values extending upto  $\delta_{10} = -35 \text{ MHz}$ . (b) Presence of L3 absorption resonance (Trace C) beyond the vertical line for  $\delta_{10} = 35 \text{ MHz}$ . Trace A in both the figures represents L2 beam transmission showing EIT for all values.

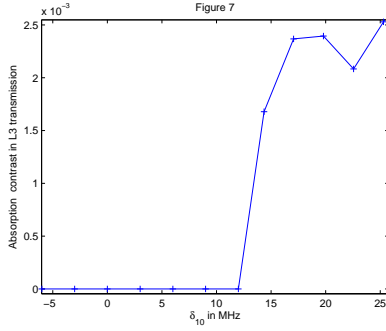


FIG. 7: Contrast of L3 absorption resonance showing a sharp threshold around  $\delta_{10} = 12 \text{ MHz}$ .

$\delta_{10}$ . Figure 6(b) shows that the narrow absorption feature in Trace C continuing for positive  $\delta_{10}$  atleast upto 35 MHz.

We have repeated the experiment with various intensities of the L2 field keeping the L3 intensity to be the same. Every time we see that there is an abrupt onset of EIT correlated absorption in L3 occurring in the vicinity of  $\delta_{10}$ . The value of  $\delta_{10}$  at which this occurs is not strongly dependent on the intensity of the L1 beam. However, the width of the absorption feature and the EIT transmission feature increase at higher intensities of L2 as expected. Plotted in Figure 7 is a typical absorption contrast of the narrow absorption in L3 as a function of  $\delta_{10}$ . We see in this figure that the absorption rises to its maximum value in a narrow range of  $\delta_{10}$ .

## A. Numerical Modeling

As seen from Figure 4, for intensities of L2 and L3 beams well within  $I_s$ , the absorption feature in L3 occurs only to the blue of  $F = 0'$ . To understand this effect we tried to model our system as a four level system with two ground levels as  $m_F = \pm 1$  ground state Zeeman sub-levels of  $5S_{1/2}, F = 1$  and two excited levels being the hyperfine levels  $5P_{3/2}, F = 0'$  and  $5P_{3/2}, F = 1'$ . The Hamiltonian consists of all the various transitions as depicted in Figure 3(d). The counter-propagating weak beam is treated perturbatively retaining terms upto first order in perturbation. This is done explicitly to separate the contribution to the density matrix elements from the forward L1 and counter L3 beams which address the same set of transitions. More importantly, off-resonant transitions are taken into account for the strong L1 beam.

We divide the total Hamiltonian into two parts.

$$H = H_0 + \Delta H \quad (1)$$

Where  $H_0$  is the Hamiltonian describing the four-level system interacting with the L1 and L2 fields.  $\Delta H$  has L3 interaction terms only. The Liouville equation for the total Hamiltonian has the form

$$\frac{d(\rho + \Delta\rho)}{dt} = -\frac{i}{\hbar}[H_0 + \Delta H, \rho + \Delta\rho] - \frac{1}{2}\{\Gamma, \rho + \Delta\rho\} \quad (2)$$

Neglecting terms which are second order in  $\Delta\rho$  and  $\Delta H$ , the above equation becomes,

$$\frac{d(\rho + \Delta\rho)}{dt} = -\frac{i}{\hbar}[H_0, \rho] - \frac{i}{\hbar}[H_0, \Delta\rho] - \frac{i}{\hbar}[\Delta H, \rho] - \frac{1}{2}\{\Gamma, \rho + \Delta\rho\} \quad (3)$$

We know that for the unperturbed system the equation

$$\frac{d(\rho)}{dt} = -\frac{i}{\hbar}[H_0, \rho] - \frac{1}{2}\{\Gamma, \rho\} \quad (4)$$

is satisfied. We proceed to find numerical solution for steady state values of  $\rho$  solving fifteen coupled equations with the constraint

$$\sum_i \rho_{ii} = 1 \quad (5)$$

We now solve the equation for  $\Delta\rho$

$$\frac{d(\Delta\rho)}{dt} = -\frac{i}{\hbar}[H_0, \Delta\rho] - \frac{i}{\hbar}[\Delta H, \rho] - \frac{1}{2}\{\Gamma, \Delta\rho\} \quad (6)$$

where the  $\rho$  values are given as inputs from the solution obtained by solving (4). Imposing the constraint,

$$\sum_i \Delta\rho_{ii} = 0 \quad (7)$$

we get 15 coupled equations for  $\Delta\rho$  which are numerically solved to obtain steady state density matrix values for the weak counter-propagating L3 field.

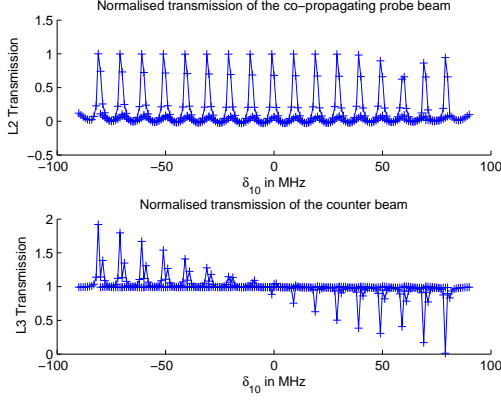


FIG. 8: Transmission of L2 and L3 for experimental parameters values as depicted in Figure 5. (a) Normalized transmission of L2 beam. (b) Normalized transmission of L3 beam

Figure 8 shows the result of our calculations. In Figure 8(a) we give the normalised transmission of the co-propagating scanned L2 beam. As expected, for all detunings  $\delta_{10}$  this shows transparency as is the case with our experimental result shown in Trace A of Figure 5. The transmission of the L3 beam is shown in 8(b). This shows gain for values of  $\delta_{10} \leq 0$ , and absorption for values of  $\delta_{10} > 0$ . This should be compared with the experimental curve for L3 transmission (Trace C) of Figure 5. While we do see absorption for values of  $\delta_{10} > 0$ , for values of  $\delta_{10} < 0$ , we do not see the theoretically predicted gain (Figure 8(b)) in our experimental curve (Trace C of Figure 5). We think that this could be due to the presence of a non-vanishing  $\pi$  component in our counter L3 beam.

### B. Threshold non-linear resonances with off-resonant interactions

It is well known that for a pure  $\Lambda$  or a double  $\Lambda$  system, in the absence of any perturbing mechanism introducing light shifts to a dark state, the system exhibits no higher order non-linearity [15]. In our system, this perturbation is introduced by the off-resonant transitions addressed by the strong L1 laser. This laser makes the transition probability for transitions of suitable velocity class of atoms, to the  $F = 1'$ , non-negligible. Our system, due to this off-resonant interaction, can be seen as modified N system as shown in Figure 3(d). So, for a suitable velocity class of atoms, there is a suppression of linear susceptibility due to EIT and a simultaneous enhancement of absorption due to higher order non-linearity to the nearby hyperfine level. This absorption due to higher order non-linearity, is distinctly seen in L3 beam due to its counter geometry. In effect, this feature is very similar to the higher order non-linear absorption seen in N systems with subnatural widths [16, 17, 18]. The difference in the present case is its strong dependence on the detuning.

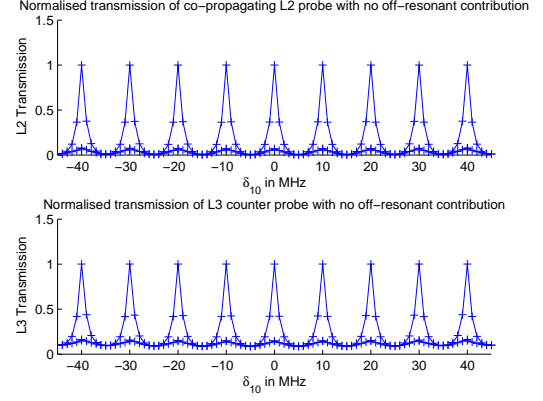


FIG. 9: Theoretical transmissions of L2 and L3 beams for experimental parameters values as depicted in Figure 5 when off-resonant contribution due to L1 laser is made zero. (a) Normalized transmission of L2 beam. (b) Normalized transmission of L3 beam

It is well known that the DTLS systems show gain [1] in some intensity regime. According to the theoretical model, since our laser addresses a DTLS there is gain due to the contribution from the double lambda part. In addition, there is also nonlinear absorption due to off-resonant interaction which is dominant. The gain becomes negligible as the laser goes beyond  $\delta_{10} = 0'$ . (Figure 8(b)). This results in absorption of L3 beam to be seen prominently, only for values of  $\delta_{01} \geq 0'$ .

We realised from our theoretical simulations that the main reason for the threshold absorption is the off-resonant addressing of  $F=1'$  level by our strong L1 beam. When we make this off-resonant contribution to be zero, then we see that both L2 and L3 transmission show increased transmission for all  $\delta_0$ , with similar widths. This is shown in Figure 9.

Both the double  $\Lambda$  and Tripod systems have shown to have many properties [19, 20, 21] which aid specific quantum engineering of superposition states [22]. Our system which is a modified double  $\Lambda$  system exhibits a threshold non-linear absorption of sub-natural width at the same frequency where transparency is seen due to ground state Zeeman coherence. The separation of absorptive and transmissive features in L2 and L3 beams is achieved by geometry of beam propagation. Such a feature is desirable from the view point of monitoring the fidelity of the dark states. Passive monitoring of counter propagating probe should reveal the nature of CPT coherence in the forward beams. Also, by using the real part of the non-linear susceptibility, one can design phase gates which work only in a specific bandwidth. In this sense, the threshold phenomenon seen here can be used as a frequency filter.



#### IV. CONCLUSIONS

We report in this paper an experimental observation of a sub-natural absorption feature in a modified N system around Zeeman degenerate transitions in the D2 manifold of  $^{87}\text{Rb}$ . This feature is seen when the gaseous Rb. atoms are irradiated with three fields all derived from the same laser. The novelty of this absorption resonance is its abrupt onset beyond a certain detuning of the laser. We show that this absorption feature in one of the beams, arises due to off-resonant absorption to the neighbouring hyperfine excited states through a higher order absorptive non-linearity. We have modeled our sys-

tem using density matrix formalism. This shows that the threshold nature of this absorption is due to a competition between gain present in such DTLs and off-resonant coherence induced absorption. This feature and its distinct appearance in only one of the three fields provides a powerful tool for frequency filtering in wave guides.

#### V. ACKNOWLEDGEMENTS

One of us, SNS thanks the Department of Science and Technology, India, for financial assistance through the WOS-A scheme.

- 
- [1] A. Lipsich, S. Barreiro, A.M. Akulshin, and A. Lezama, Phys. Rev. A **61** 053803 (2000).
  - [2] A.M. Akulshin, S. Barreiro and A. Lezama, Phys. Rev. A **57** 2996 (1998)
  - [3] A. Lezama, S. Barreiro, A. Lipsich, and A. M. Akulshin, Phys. Rev. A **61** 013801 (1999).
  - [4] A. Lezama, S. Barreiro, and A. M. Akulshin, Phys. Rev. A **59** 4732 (1999).
  - [5] F. Renzoni, W. Maichen, L. Windholz, and E. Arimondo, Phys. Rev. A **55** 3710 (1997).
  - [6] G Wasik, W Gawlik, J Zachorowski and Z Kowal, Phys. Rev. A **64** 051802(R) (2000).
  - [7] S. Haroche and F. Hartmann, Phys. Rev. A **6** 1280 (1972); C. Affolderbach, S. Knappe, R. Wynands, A. V. Taichenachev and V. I. Yudin, Phys. Rev. A **65** 043810 (2002).
  - [8] A. V. Taichenachev, A. M. Tumaikin, and V. I. Yudin, Phys. Rev. A **61** 011802 (R) (1999).
  - [9] C. Goren, A. D. Wilson-Gordon, M. Rosenbluh and H. Freidmann, Phys. Rev. A **72** 023826 (2005); *ibid*, **70** 043841 (2004); *ibid*, **69** 053818 (2004); *ibid* **67** 033807 (2003).
  - [10] G. Ban, V. Lorent and A. Lezama, Phys. Rev. A **67** 043810 (2003).
  - [11] Y. Gu, Q. Sun, Q. Gong, Phys. Rev. A **69** 063805 (2004).
  - [12] R. W. Boyd, M. G. Raymer, P. Narum and D. J. Harter, Phys. Rev. A **24** 411 (1981).
  - [13] A. Narayanan, A. Sharma, Preethi T.M, A. Hazra and H. Ramachandran, accepted for publication in Canadian Journal of Physics.
  - [14] A. Hazra, A. Narayanan and S.N. Sandhya, Poster presentation at *ICAP 2008*, Storrs, Connecticut (2008).
  - [15] S. Rebic, D. Vitali, C. Ottaviani, P. Tombesi, M. Artoni, F. Cataliotti, and R. Corbalan, Phys. Rev. A., **70**, 032317 (2004)
  - [16] S. Zibrov, I. Novikova, D. F. Phillips, A. V. Taichenachev, V. I. Yudin, R. L. Walsworth and A. S. Zibrov, Phys. Rev. A, **72**, 011801(R) (2005)
  - [17] A.S. Zibrov, C.Y. Ye, Y. V. Rostovtsev, A. B. Matsko, and M. O. Scully, Phys. Rev. A, **65**, 043817 (2002)
  - [18] C. Y. Ye, A. S. Zibrov, Yu. V. Rostovtsev, and M. O. Scully, Phys. Rev. A, **65**, 043805 (2002).
  - [19] D. Petrosyan and Y P.Malakyan, Phys. Rev. A, **70**, 023822, (2004)
  - [20] A. M. Akulshin, A I Sidorov, R.J McLean and P Hannaford, J. Opt.B, **6** 491 (2004)
  - [21] Y Han, J Xiao, Y Liu, C Zhang, H Wang, Min Xiao, and K Peng, Phys. Rev. A, **77**, 023824 (2008)
  - [22] F Vewinger, M Heinz, R G Fernandez, N V. Vitanov, and K Bergmann, Phys. Rev. Lett., **91**, 213001 (2003).
  - [23] Excited hyperfine states are shown primed